Generation of Morphological Models of Atherosclerotic Arteries from High Resolution MR images

M. Auer[1], R. Stollberger[2], P. Regitnig[3], G. A. Holzapfel[1], F. Ebner[4]

[1]Graz University of Technology, Institute for Structural Analysis – Computational Biomechanics, Graz, Austria, [2]LKH - Universitätsklinikum Graz, Abteilung für klinische und Experimentelle Magnetresonanzforschung, Graz, Austria, [3]Karl-Franzens-University Graz, Institute of Pathology, Graz, Austria, [4]LKH - Universitätsklinikum Graz, Klinischen Abteilung für Neuroradiologie, Universitätsklinik für Radiologie, Graz, Austria

Introduction

To date, mechanical investigations of diseased arterial walls are based on over-simplified geometrical models, which are inconsistent with histological evidence. Crucial prerequisites for meaningful stress-strain analyses of atherosclerotic arteries are, however, appropriate morphological models that represent the three-dimensional boundary surfaces of histologically and mechanically distinct major components of the diseased wall. The assessment of the arterial wall structure is an issue of highest clinical priority. In recent years, however, rapid progress in the development of high-resolution MR imaging allows a not-destructive view of the 'anatomy' of atherosclerotic lesions with high tissue contrast. The present *in vitro* study is aimed to create morphological models from multi-phasic high-resolution MR images. These models represent both the three-dimensional geometry and the histological nature of major tissue components of diseased arteries.

Methods

Diseased iliac arteries from diseased humans (> 50 years) were excised during autopsy within 24 hours of death. Use of autopsy material from human subjects was approved by the Ethics Committee, Medical University Graz, Austria. Special 3D Turbo Spin Echo sequences provided PD, T2 and T1-weighted images of the specimen with high spatial resolution (0.23mm lateral and 0.60mm axial), see Figs. 1(a)-(c). We apply the well known N3 (**N**onparametric **N**onuniform intensity **N**ormalization), in order to correct the intensity inhomogeneities. In addition, we use the so-called edge/flat/gray (EFG)-filter, which is an edge preserving filter. After these preprocessing operations the image quality is improved significantly, see Fig. 1(d). Active contour-based models, also known as "snakes", are used to segment the image into predefined components. In our segmentation, we distinguish between 8 components. In particular, we segment the arterial wall into three sections: the adventitia, the media, and the intima, and distinguish between diseased and non-diseased components. Additionally, there appear calcifications and lipid pools in the intima. Since we are segmenting 3D volume data, it is straightforward to use a 3D-snake model, which is based on serially linked 2D-snakes. These snakes can only move in the x,y-directions and not in the axial (z) direction.

The segmentation of the arterial wall and it's components is performed in several steps. First, we initialize the snake outside the **R**egion **o**f **I**nterest (ROI) and find so the outer boundary of the adventitia. Next, we use the boundary of the adventitia to find the center of the lumen, by using an automatic threshold method. Then, we initialize a snake around the center of the lumen. These two snakes are used to detect both outer wall boundaries, see Fig. 2(a). Now we are detecting the calcifications by an automatic threshold method and enhance the selected regions by morphological operations. A further snake is then placed on the boundaries of the selected calcified regions in order to enhance the accuracy of the boundaries. In a next step we separate diseased from non-diseased wall sections. Therefore, we search for the position with the thinnest wall thickness and consider this wall segment as non-diseased, see the dark boundaries in Fig. 2. Wall segments, which are thicker than 150% of the non-diseased wall are considered as diseased segments. The detection of the last two boundaries (adventitia-media and media-intima boundaries) is more difficult, because of the low contrast and, consequently, the low intensity gradient. Therefore, we need a good initial estimation of these boundaries. For that reason, we consider morphological knowledge and statistical wall thickness of these wall components. For example, the media must be located behind calcifications, and may become a fraction of the normal (non-diseased) wall thickness. In non-diseased regions we initialize the boundaries based on the known statistical wall thickness. After the initialization we perform the movement of the two snake boundaries simultaneously and ensure that the wall-thicknesses do not vary too much from the known wall thicknesses. The boundaries of all components are described with NURBS (**N**on **U**niform **R**ational **B**-**S**plines), which provide analytical descriptions of the 3D geometries. Hence, the geometrical description using NURBS allows straightforward mesh refinements for subsequent finite element analyses.

Results

High resolution magnetic-resonance images show the complex structure of atherosclerotic lesions (Fig. 1(a)-(c)). In particular, the adventitia appears as a homogeneous dark layer, while the media is a relatively bright layer. Calcifications appear as very dark areas within the intima and can be determined using appropriate image processing algorithms based on thresholding. Lipid pools have a higher gray-level variance. Fibrotic intima show bright gray-levels. The proposed methodology yields highly resolved multi-component models of diseased arteries (Fig. 3). Each of the segmented components is represented by an individual geometrical model. The performance of our algorithm was tested by comparing the automatic detected boundaries with the result of two individual human experts. The mean distance error was less than 1 pixel (0.23mm). The association of segmented tissue components provides an excellent basis for computational (finite element) stress-strain analysis.

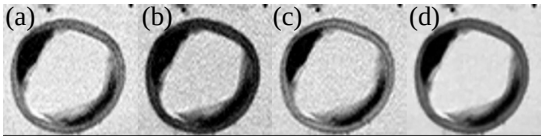

Figure 1. *Raw MR-images: PD (a), T2 (b), T1(c), and preprocessed image (d).*

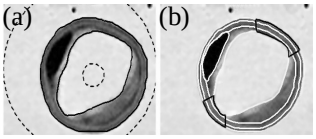

Figure 2. *Initial (dashed line) and final (solid) boundaries of the wall using snakes (a); final segmentation result (b).*

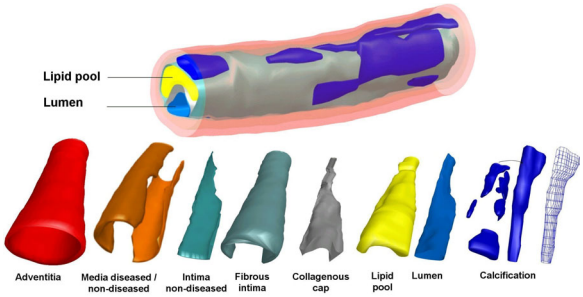

Figure 3. *3D reconstruction of a high-grade stenosis at the top; different wall and plaque components are shown at the bottom.*